Magnetooptical investigations of the noncollinear state induced in antiferromagnetic cobalt fluoride by a longitudinal magnetic field

N. F. Kharchenko, V. V. Eremenko, and L. I. Belyĭ

Physicotechnical Institute of Low Temperatures, Ukrainian Academy of Sciences
(Submitted 28 August 1981)
Zh. Eksp. Teor. Fiz. **82**, 827–843 (March 1982)

The spin-orientational transition of the tetragonal two-sublattice antiferromagnetic CoF_2 (characterized by a large single-ion rhombic magnetic anisotropy) to a noncollinear state under the action of a longitudinal magnetic field $H \| C_4$ is investigated by magnetooptical methods. The absence of discontinuities in the plots of the linear birefringence and Faraday rotation of light propagating along the C_4 axis indicates the absence of a phase transition of the spin-flop type. The presence of kinks on the curves indicates that the noncollinear canted state is induced smoothly by the magnetic field $H \| C_4$. It is shown that the sample destruction observed in a strong magnetic field in this study and earlier, is not due to spin-flop stratification of the sample into magnetic domains of the various phases but to the antiferromagnetic (AFM) inhomogeneity of the sample, i.e., to the presence of 180-degree AFM domains. From the dependence of the optical axes of the AFM crystal in the noncollinear state on the magnetic field intensity it is concluded that this state has the magnetic symmetry $\underline{2/m}$. The behavior of the magnetic system of a tetragonal AFM with account taken of single-ion rhombic anisotropy is analyzed phenomenologically for various models of variation of the lengths of the sublattice magnetic-moment vectors in the noncollinear state.

PACS numbers: 78.20.Ls, 75.50.Ee, 75.30.Gw, 75.60.Ch

1. INTRODUCTION

We present here the results of an investigation of the magnetic state of a two-sublattice tetragonal antiferromagnet (AFM), namely cobalt fluoride, in a longitudinal magnetic field. Cobalt fluoride is a typical representative of collinear tetragonal AFM, whose thermodynamic potential can contain a Dzyaloshinskiĭ invariant, of the type $D(m_x l_x + m_y l_y)$, due to the rhombic symmetry of the ligand environment of the magnetic ion.[1] This invariant manifests itself when the sublattice moments deviate from the longitudinal orientation $\mathbf{M}_i \| C_4$, and its influence is substantial for spin-orientational transitions in a magnetic field.[2] At $D \neq 0$ in a longitudinal magnetic field $H \| C_4$, the spin-flop state with polar angle $\theta = \pi/2$ of the AFM vector can no longer be realized. Moreover, at $D \geq D_{cr}$ the transition to the canted ($\theta \neq \pi/2$) noncollinear state cannot be of first order.

The possibility of a smooth transition into a noncollinear state in crystals of this type was confirmed by spectral investigations of iron fluoride in longitudinal pulsed fields.[3] In the CoF_2 crystal, however, which has a larger low-symmetry single-ion anisotropy, experiments in a longitudinal magnetic field revealed a radical change in the state of the crystal, which led to destruction of the sample.[4-7] It was assumed that the crystal undergoes a first-order phase transition of the spin-flop type, and the magnetic phase stratification in the transition leads to destruction of the sample. Estimates show, however, that such an abrupt magnetic transition is impossible in this crystal. Indeed, the parameters of the exchange ($2H_E = 500$–700 kOe) and axial ($H_A = 100$–300 kOe) interaction[4-7] yield, according to the phenomenological expression[2]

$$H_{D_{cr}} \approx \tfrac{1}{2} H_A [H_A (2H_E + H_A)]^{1/2} (H_E + H_A)^{-1},$$

a rhombic-anisotropy critical field 80 ± 50 kOe. Phenomenological estimate of H_D, based on the results of ex-

periments on the results of experiments on the behavior of the magnetic system of CoF_2 in transverse fields,[4,8] yield a value of H_D in the interval 170 ± 70 kOe. Quantum-mechanical calculations of the longitudinal magnetic susceptibility and of the antiferromagnetic-resonance spectra call for still larger values of H_D.[9,10] According to these estimates $H_D \geq H_{D_{cr}}$ and the transition to the noncollinear state at $H \| C_4$ can be smooth. Even if the transition does remain of first order, the differences between the collinear and canted states should be small. It is difficult to expect that magnetic stratification of two phases having close parameters into domains would destroy the sample.

At the same time, the possible cause of the destruction may be elastic stresses produced in certain domain walls between the 180° AFM domains in a longitudinal magnetic field on account of linear magnetostriction. The linear magnetostriction $H^{-1}\Delta l'/l$ ($\Delta l/l$ is the relative change of the sample thickness in the field H) reaches in CoF_2 a value $\sim 10^{-10}$ Oe^{-1} (Ref. 11) and can lead in a field of $\sim 10^5$ Oe to elastic stresses in an incoherent domain wall of thickness $h = 10^{-5}$ cm which separates AFM domains having along [110] an approximate size 10^{-1} cm, equal in order of magnitude to $(\Delta l/h)\sigma_{\text{shift}} \sim 0.1\sigma_{\text{shift}}$. Therefore the question of the order of the spin-orientational transition remain open.

To study the magnetic states of the crystal, we resorted to the magnetooptical methods of Faraday rotation (FR) and linear birefringence (LB). The fact that circular birefringence is proportional to the projection of the magnetization of the AFM, while the linear birefringence is connected with projections of the magnetic moments of the sublattices in a more complicated manner, gave ground for hoping to obtain additional information in the behavior of the magnetic system of CoF_2. In addition, the recently observed longitudinal linear magnetooptical effect (LMOE) in this crystal[12]

made it possible to distinguish visually between 180° AFM domains and to monitor the AFM domain structure of the sample. The experiments were performed with a single-domain sample. This circumstance turned out to be very important in the protection of the sample against damage.

2. PHENOMENOLOGICAL DESCRIPTION OF THE CRYSTAL-OPTICAL PROPERTIES OF THE ANTIFERROMAGNET CoF$_2$ IN A MAGNETIC FIELD

The magnetooptical properties of tetragonal AFM with magnetic Laue groups $\underline{4}$ and $\underline{422}$, which include the CoF$_2$ crystal, can differ significantly from the properties of other uniaxial AFM. A longitudinal linear magnetooptical effect is allowed in them, and the crystals become optically biaxial in a magnetic field H ∥ C_4. The optical birefringence which appears in the direction of the former optical axis is elliptic, for in this case the influence of the magnetootpic Faraday effect is unavoidable. It is expedient to represent it as a sum of two effects, namely magnetic-circular and linear birefringences, described separately by anti-symmetrical and symmetrical components ε_{ij}^a and ε_{ij}^s. This separation is possible by virtue of the validity of the superposition principle, according to which the action of an elliptically birefringent plate is equivalent to the action of a set of alternating only linearly and only circularly birefringent plates.[13] The superposition principle is satisfied accurate to the ratio $(\varepsilon^a/\varepsilon^s)^2 \sim 10^{-8}$. Hereafter, the terms "circular birefringence" (or FR) and "linear birefringence" (birefringence of linearly polarized light) must be understood within the framework of the foregoing separation of the effects. The optical indicatrix of the crystal assumes a similar meaning, being a geometric representation of only the symmetrical part of the dielectric tensor. We consider briefly the changes of the optical properties of the CoF$_2$ crystal, which can accompany its magnetic phase transitions.

The magnetic point groups of the field-induced possible magnetic states constitute those subgroups of the point group of the AFM CoF$_2$ crystal $\underline{4/mmm}$, which admit of the existence of a projection of the axial vector along H. Considering only those magnetic structures in which the magnetic cell is equal to the crystal cell, it can be seen that it is possible to induce two types of noncollinear structures, characterized by the groups $\underline{2/m}$ and $\overline{1}$. The group $\underline{2/m}$ describes noncollinear, canted ($\theta \neq \pi/2$) and spin-flop ($\theta = \pi/2$) states in which the sublattice moments are located in a diagonal crystal plane of the type (110). The group $\overline{1}$ describes the canted and spin-flop states with sublattice moments lying in arbitrary planes, including a state with an AFM vector 1 in the (100) plane. We note that the (100) plane is no longer a symmetry plane in a field H ∥ C_4.

The dependences of the components of the dielectric tensor $\varepsilon_{ij} = \varepsilon_{ij}^s + \varepsilon_{ij}^a$ on the magnetic-field intensity can be represented in the form

$$\varepsilon_{ij}^s(A_\nu) = \varepsilon_{ij0}^s(A_\nu) + q_{ij\alpha}(A_\nu)H_\alpha + c_{ij\alpha\beta}(A_\nu)H_\alpha H_\beta + \ldots,$$

$$\varepsilon_{ij}^a(A_\nu) = \varepsilon_{ij0}^a(A_\nu) + f_{ij\alpha}(A_\nu)H_\alpha + e_{ij\alpha\beta}(A_\nu)H_\alpha H_\beta + \ldots . \quad (1)$$

The matrices of the tensors $q_{ij\alpha}$ and $c_{ij\alpha\beta}$ for different magnetic states have, in abbreviated notation, the form:

1) collinear AFM state $4/m\underline{mm}$, $z \parallel [001] \parallel \underline{4}$, $x \parallel [100] \parallel \underline{2}$:

$$q_{ij\alpha} \sim \begin{vmatrix} 0 & 0 & 0 \\ 0 & 0 & 0 \\ 0 & 0 & 0 \\ q_{41} & 0 & 0 \\ 0 & q & 0 \\ 0 & 0 & q_{63} \end{vmatrix}, \quad c_{ij\alpha\beta} \sim \begin{vmatrix} c_{11} & c_{12} & c_{13} & 0 & 0 & 0 \\ c_{12} & c_{11} & c_{13} & 0 & 0 & 0 \\ c_{31} & c_{31} & c_{33} & 0 & 0 & 0 \\ 0 & 0 & 0 & c_{44} & 0 & 0 \\ 0 & 0 & 0 & 0 & c_{44} & 0 \\ 0 & 0 & 0 & 0 & 0 & c_{66} \end{vmatrix}; \quad (2)$$

2) noncollinear state $\underline{2/m}$, $z' \parallel 4$, $x' \parallel [110] \parallel \overline{2}$:

$$q_{ij\alpha} \sim \begin{vmatrix} q_{11} & 0 & q_{13} \\ q_{21} & 0 & q_{23} \\ q_{31} & 0 & q_{33} \\ q_{11} & 0 & q_{43} \\ 0 & q_{52} & 0 \\ 0 & q_{62} & 0 \end{vmatrix}, \quad c_{ij\alpha\beta} \sim \begin{vmatrix} c_{11} & c_{12} & c_{13} & c_{14} & 0 & 0 \\ c_{21} & c_{22} & c_{23} & c_{24} & 0 & 0 \\ c_{31} & c_{32} & c_{33} & c_{34} & 0 & 0 \\ c_{11} & c_{42} & c_{13} & c_{44} & 0 & 0 \\ 0 & 0 & 0 & 0 & c_{55} & c_{56} \\ 0 & 0 & 0 & 0 & c_{65} & c_{66} \end{vmatrix}; \quad (3)$$

3) noncollinear state $\overline{1}$: all the tensor components differ from zero.

It is seen from (2) and (3) that in the case of collinear AFM configuration and H ∥ C_4 the manifestations of the linear and quadratic magnetooptic effects are different. The quadratic effect preserves the symmetry of the characteristic surface of the tensor ε_{ij}^s, since the off-diagonal components of the tensor, which are proportional to H_i^2, are absent. The linear effect, however, leads to rotation of the tensor axis and to a lowering of its symmetry—a component ε_{xy}^s appears in the field. In noncollinear configurations, the linear and quadratic magnetooptical effects cause changes in the identical components ε_{ij}^s. The crystal-optical properties of the collinear and the possible noncollinear states are different. In the collinear state $\underline{4/mmm}$ the indicatrix axes are rigidly tied to the crystallographic axes: $\overline{n}_3 \parallel [001]$, $n_2 \parallel [110]$. The optical axes lie in one of two diagonal planes of the (110) type, depending on the sign of the z-projection of the AFM vector and on the direction of the magnetic field. Substantial qualitative differences can exist between the indicatrix axes in the noncollinear states $\underline{2/m}$ and $\overline{1}$. In the state $\underline{2/m}$ the two indicatrix axes are located in a plane of the type (110), but the n_3 axis is no longer parallel to [001] and is rotated about the axis $x' \parallel [110]$ through an angle

$$\text{tg}\,2\xi_{x'} = 2\varepsilon_{y'z}^s(\varepsilon_{y'y'}^s - \varepsilon_{x'x'}^s)^{-1}.$$

The angle $\xi_{x'}$ is small, since $\varepsilon_{y'z}^s \ll (\varepsilon_{y'y'}^s - \varepsilon_{x'x'}^s)$. In the state l, the axes have a common position. The azimuthal angle of the plane of the indicatrix axes n_3 and n_2 (and of the plane of the optical axes), reckoned from the [110] direction, may be not small, since the changes of the off-diagonal ($\varepsilon_{x'y'}^s$) and the diagonal ($\varepsilon_{x'x'}^s$ and $\varepsilon_{y'y'}^s$) components are due to magnetooptical effects and are quantities of the same order. We note that it should not coincide with the azimuth of the plane in which the magnetic moments are located.

The magnetic states have different numbers of nonzero components ε_{ij}^a. The qualitative difference between the properties governed by ε_{ij}^a, however, can manifest itself only at a transverse experimental geometry, k ⊥ [001], at which the measurement of the

small FR is made difficult by the large natural linear birefringence.

Thus, the foregoing analysis demonstrates the possibility of determining the symmetry of the strong-field magnetic state of the CoF_2 crystal with the aid of crystal-optical methods.

For a more detailed analysis of the behavior of the optical properties upon rearrangement of its magnetic structure, it is convenient to express the components of the tensor ε_{ij}^s in terms of the projections of the magnetic vectors, by considering them as an external action on the crystal. This approach makes it possible to connect quantitatively the magnetooptical effects with the projections of the magnetic vectors. Confining ourselves to quadratic and linear terms in m and l for an AFM of the type $4_d^-2_d^+$, we can write:

$$\varepsilon_{ij}' = \varepsilon_{ij0}^s + Q_{ijrs}^{ll}l_rl_s + Q_{ijrs}^{ml}m_rl_s + Q_{ijrs}^{mm}m_rm_s, \tag{4}$$

where the matrices of the tensor Q_{ijrs} take in abbreviated notation the form

$$Q_{\mu\nu}^{ll} \sim Q_{\mu\nu}^{mm} = \begin{vmatrix} Q_{11} & Q_{12} & Q_{13} & 0 & 0 & 0 \\ Q_{12} & Q_{11} & Q_{13} & 0 & 0 & 0 \\ Q_{31} & Q_{31} & Q_{33} & 0 & 0 & 0 \\ 0 & 0 & 0 & Q_{44} & 0 & 0 \\ 0 & 0 & 0 & 0 & Q_{44} & 0 \\ 0 & 0 & 0 & 0 & 0 & Q_{66} \end{vmatrix},$$

$$Q_{\mu\nu}^{ml} = \begin{vmatrix} 0 & 0 & 0 & 0 & 0 & Q_{16} & 0 & 0 & Q_{19} \\ 0 & 0 & 0 & 0 & 0 & Q_{19} & 0 & 0 & Q_{16} \\ 0 & 0 & 0 & 0 & 0 & Q_{36} & 0 & 0 & Q_{36} \\ 0 & 0 & 0 & 0 & Q_{15} & 0 & 0 & Q_{18} & 0 \\ 0 & 0 & 0 & Q_{45} & 0 & 0 & Q_{18} & 0 & 0 \\ Q_{61} & Q_{61} & Q_{63} & 0 & 0 & 0 & 0 & 0 & 0 \end{vmatrix}. \tag{5}$$

The contraction of both pairs of symmetrical indices $ij \to \mu$, $rs \to \nu$ is contravariant for the components of the tensors Q_{ijrs}^{ll} and Q_{ijrs}^{mm} ($Q_{ijrs} = Q_{\nu\mu}$) and covariant for the dyads $l \cdot l$ and $m \cdot m$ [$l_rl_s = (ll)_\nu$ at $r=s$ and $l_rl_s = 2(ll)$ at $r \neq s$]. The form of the contraction in a more rigorous notation[20] is $Q_{ijrs} = Q^{\mu\nu}(ll)_\nu$. The contraction of the indices of the components of Q_{ijrs}^{ml} and of the dyad $m \cdot l$ was carried out in accordance with the rule $Q_{ijrs}^{ml} = Q^{ml}$ and $m_rl_s = (ml)$ for all i, j, r, and s. The connection between the nonsymmetrical indices r and s and the index ν is the following:

rs:	11	22	33	23	13	12	32	31	21
ν:	1	2	3	4	5	6	7	8	9

Expanding (5), we write expressions (4) in expanded form:

$$\varepsilon_{xx}' = \varepsilon_{xx0}' + Q_{11}^{ll}l_x^2 + Q_{12}^{ll}l_y^2 + Q_{13}^{ll}l_z^2 + Q_{11}^{mm}m_x^2 + Q_{12}^{mm}m_y^2 + Q_{13}^{mm}m_z^2 + Q_{16}^{ml}m_xl_y + Q_{19}^{ml}m_yl_x,$$
$$\varepsilon_{yy}' = \varepsilon_{yy0}' + Q_{12}^{ll}l_x^2 + Q_{11}^{ll}l_y^2 + Q_{13}^{ll}l_z^2 + Q_{12}^{mm}m_x^2 + Q_{11}^{mm}m_y^2 + Q_{13}^{mm}m_z^2 + Q_{19}^{ml}m_xl_y + Q_{16}^{ml}m_yl_x,$$
$$\varepsilon_{zz}' = \varepsilon_{zz0}' + Q_{31}^{ll}(l_x^2 + l_y^2) + Q_{33}^{ll}l_z^2 + Q_{31}^{mm}(m_x^2 + m_y^2) + Q_{33}^{mm}m_z^2 + Q_{36}^{ml}(m_xl_y + m_yl_x), \tag{6}$$
$$\varepsilon_{yz}' = Q_{44}^{ll}l_yl_z + Q_{44}^{mm}m_ym_z + Q_{45}^{ml}m_zl_x + Q_{48}^{ml}m_xl_z,$$
$$\varepsilon_{xz}' = Q_{44}^{ll}l_xl_z + Q_{44}^{mm}m_xm_z + Q_{45}^{ml}m_yl_z + Q_{48}^{ml}m_zl_y,$$
$$\varepsilon_{xy}' = Q_{66}^{ll}l_xl_y + Q_{66}^{mm}m_xm_y + Q_{61}^{ml}(m_xl_x + m_yl_y) + Q_{63}^{ml}m_zl_z.$$

Here $x \parallel [100]$ and $z \parallel [001]$. We note that the coefficients $Q_{\mu\nu}^{mm}$ and $Q_{\mu\nu}^{ll}$ are equal to each other if they are due only to optical electronic transitions within the limits of a single sublattice.

We consider now the behavior of ε_{ij}^s and of the optical properties of CoF_2 as functions of the projections m_r and l_s in different magnetic states.

Collinear AFM state

At a fixed direction $H \parallel C_4$, only two components $m_z = \chi_{xx}H_z$ and l_z are different from zero and lead to the appearance of an off-diagonal component

$$\varepsilon_{xy}' = Q_{63}^{ml}m_zl_z. \tag{7}$$

Since the remaining off-diagonal components ε_{ij}^s remain unchanged, the optical axes of the crystal, as already mentioned, lie in a plane of the type (110). The bisector of the angle between them is directed along [001]. The birefringence for light propagating along [001] is given by

$$n_1 - n_2 = \frac{1}{\tilde{n}} \text{ sign } l_z \text{ sign } H_z Q_{63}^{ml} \chi_{zz}|l_z|H. \tag{8}$$

Noncollinear state $2/m$

The nonzero transverse projections of m and l are pairwise equal: $m_x = \pm m_y = \pm 2^{-1/2}m_\perp$ and $l_x = \pm l_y = \pm 2^{-1/2}l_\perp$. The changes of the transverse diagonal components of ε_{ij}^s are equal to one another: $\Delta\varepsilon_{xx}^s = \Delta\varepsilon_{yy}^s$. Also equal are the moduli of the off-diagonal components: $|\varepsilon_{xx}^s| = |\varepsilon_{yz}^s|$. The indicatrix axes n_1 and n_2 lie as before in a plane of the type (110). but the n_3 axis is rotated in this plane through a small angle $\xi_{x'}$ defined by the relation

$$\text{tg } 2\xi_{x'} \approx \frac{4\sqrt{2}(Q_{44}^{ll}l_zl_z + Q_{44}^{mm}m_zm_z + Q_{45}^{ml}m_yl_z + Q_{48}^{ml}m_zl_y)}{\varepsilon_{\nu\nu0}' - \varepsilon_{zz0}'}. \tag{9}$$

The magnitude and sign of $\xi_{x'}$ depend on the magnitudes and signs of the projections m_x. m_y. l_x. l_y. m_z. and l_z. When the direction of the field is reversed. the angle $\xi_{x'}$ changes. The angle $\xi_{x'}$ is different also for two AFM domains. It is seen from (9) that if $m_\perp$ and l_z are zero (spin flop state). the angle $\xi_{x'}$ does not vanish.

Noncollinear state $\overline{1}$

In this case, as can be seen from (6). the position of indicatrix axes n_1 and n_2 is arbitrary. The angle between the n_1 axis and [110] can assume arbitrary values in the general case of the orientation l. Even if we consider states in which l and m lie in planes close to the type (100), then the angles of rotation of the axes n_1 and n_2 them relative to the planes (100) and (010), can differ substantially from 0° in the presence of longitudinal projections m_z and l_z:

$$\text{tg } 2\xi_z$$
$$\approx \frac{2[Q_{63}^{ml}m_zl_z + Q_{66}^{ll}l_xl_y + Q_{66}^{mm}m_xm_y + Q_{61}^{ml}(m_xl_x + m_yl_y)]}{(Q_{11}^{ll} - Q_{12}^{ll})(l_x^2 - l_y^2) + (Q_{11}^{mm} - Q_{12}^{mm})(m_x^2 - m_y^2) + (Q_{16}^{ml} - Q_{19}^{ml})(m_xl_y - m_yl_x)}. \tag{10}$$

Only in the spin-flip state ($l_z = 0$) does the angle ξ_z vanish, i.e., the plane of the optical axis coincides with a plane of the type (100), namely the plane of the magnetic moments. The small angle between n_3 and [001] does not vanish in the spin-flop state. At $l \parallel [100]$, the axis n_3 is rotated around the axis $x \parallel [100]$ through an angle

$$\text{tg } 2\xi_x \approx \frac{Q_{44}^{mm}m_\perp m_z + Q_{48}^{ml}m_zl_\perp}{\varepsilon_{\nu\nu0}' - \varepsilon_{zz0}'}. \tag{11}$$

492   Sov. Phys. JETP 55(3), March 1982

Kharchenko et al.   492

The foregoing analysis shows that the magnetooptical properties of a tetragonal AFM of the type $4_z^- 2_z^- 2_d^-$ depend significantly on the symmetry of the strong-field state in the AFM-vector direction, and can be used to study these states. We describe below the results of experimental magnetooptical investigations of the behavior of the magnetic structure CoF_2 in pulsed magnetic fields.

3. EXPERIMENTAL PROCEDURE AND RESULTS

We used the method of observing conoscopic figures, which made it possible to determine clearly and unambiguously the azimuth Φ of the plane of the optical axes and the angle $2V$ between the optical axes. In addition, we determined the linear and circular birefringences. To this end we measured the additional angular parameters of the first isochromates of the conoscopic figure. The use of circular polarized light made it possible to decrease to a minimum the influence of the magnetic circular birefringence when determining the positions of the optical axes.

The general diagram of the setup is shown in Fig. 1. The sample was secured to a cold finger located in a vacuum cavity inside a pulsed solenoid with a working opening of approximately 4 mm. Inside the solenoid, on both sides of the sample, were located two lenses, L_1 and L_2 with approximate focal lengths 5 mm. The focal planes of the lenses coincided with the location of the sample. The lenses made it possible to work with a light cone having an approximate apex angle 20°. The optical axes of the lenses and of the crystal coincided with the geometric axis of the solenoid within approximately 2°. The image of the conoscopic figure was projected by lens L_3 on the plane of the photographic film. The light from the flashlamp was synchronized with the maximum of the magnetic-field pulse. The rise time of the field pulse $3 \cdot 10^{-3}$ sec was much longer than the duration of the light pulse $5 \cdot 10^{-6}$ sec. One light flash was sufficient to photograph the conoscopic picture through light filters SZS-22 and SS-4, which separated, with allowance for the spectral characteristics of the photographic emulsion and for the emission spectrum of the CoF_2 crystal, a spectral region near 4000 Å with a half-width not larger than 200 Å. The circular polarizers were combinations of a linear dichroic polaroid and a quarter-wave mica plate. In addition to photohraphy, we used also photoelectric registration of narrow light beams whose directions were close to the bisector of the optical axis and were monitored by observing the conoscopic figures. In addition to circularly polarized light, we used also linearly polarized light, particularly when investigating the behavior of a multidomain sample.
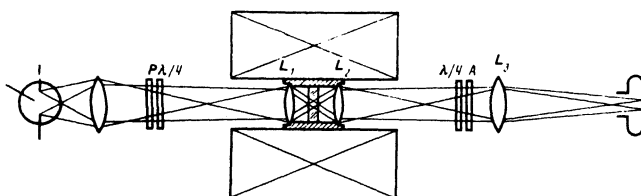
The homogeneity of the AFM structure of the sample could be monitored in fields $H < H_{cr}$ against the birefringence induced by a magnetic field $H \parallel [001]$. By varying the methods of securing the sample it was possible to control, to a certain degree, the AFM domain structure of the sample. Securing the sample to the cold finger by BF adhesive led to a multidomain structure. The conoscopic picture of such a sample is close to uniaxial even in 100 kOe fields. Mutual cancellation of the linear birefringence by AFM domains located one after the other made it possible to measure in the usual manner the Faraday rotation of the linearly polarized light. As a rule, fields close to H_{cr} (but not necessarily equal to H_{cr}), damaged the multidomain sample.

Deformation of the sample in the [110] direction makes the AFM of the sample single-domain in a magnetic field $H \parallel [001]$, owing to the piezomagnetic effect. At small volumes of the solenoid, we chose a pressure that ensured the required strains in the [110] direction. The pressure on the sample placed in the capsule was produced by inserting liners between the sample and the capsule wall. A conoscopic method was used to monitor the single-domain character of the sample. In a field weaker than 100 kOe, the sample went over into a state close to the single-domain AFM state. This state was preserved during repeated actions of a pulsed field of intensity up to 250 kOe. Measurement of the linear birefringence $(n_m - n_p)$ in a field $H < 182$ kOe yielded for the slope of the linear dependence of the birefringence on H a value of approximately $7 \cdot 10^{-7}$ kOe^{-1}, close to the $9 \cdot 10^{-7}$ kOe^{-1} obtained for a homogeneous sample.[12] All the measurements in a field $H > H_{cr}$ were performed at a single direction of the field.

To determine the linear and circular birefringences, the conoscopic figures were used to determine the relations between the birefringence and the angle $2V$ between the optical axes and with the angular distance U between the optical axis and a line passing through the isochromate and equidistant from the optical axes. The following relations are valid at $V, U \ll 1$:

$$n_m - n_p = \frac{\lambda}{t}\left(\frac{V}{U}\right)^{1/2}, \quad n^+ - n^- = \frac{\lambda}{t}\left[1 - \left(\frac{U}{U_0}\right)^4\right]^{1/2}.$$

Here λ is the wavelength of the light, t is the thickness of the plane-parallel plate, U_0 is the value of the angle U in the absence of circular birefringence, and n_p, n_m and n_g are the smallest, average, and largest refractive indices. Under the condition $[(n_g - n_p) - (n_{g_0} - n_{p_0})] \times (n_{g_0} - n_{p_0})^{-1} \ll 1$, which is usually satisfied (n_{p_0} and n_{g_0} are the refractive indices in the absence of a field), we have $U_0 = U(H = 0)$.

Figure 2 demonstrates the change of the conoscopic figures of the investigated sample with increase of the intensity of the field $H \parallel [001]$. It is seen from the photographs that the angle between the optical axes first increases with increasing field, and then decreases. In addition, it is seen that the plane of the optical axes is close to (110) at all values of the field. Visual and photometric methods were used to determine
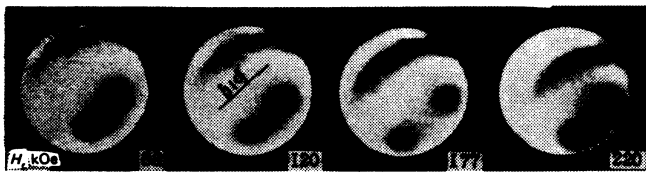

FIG. 1. Setup for the measurement of birefringence of light by the method of conoscopic figures in a pulsed field.

FIG. 2. Change of the conoscopic figures of CoF_2 as a function of the magnetic field intensity $H \parallel C_4$, $\lambda \approx 4000$ Å, $T = 11$ K, $t = 0.64$ mm.

FIG. 4. Dependence of the azimuthal angle of the plane of the optical axis on the intensity of the field $H \parallel C_4$.

the positions of the optical axes and of the isochromates. With increasing H, the error in the determination of the directions of the optical axes increases because the ellipticity of the optical modes propagating in directions close to the optical axes increases as a result of the increase of the circular birefringence. Figure 3a and 3b show the obtained linear birefringence δ and Faraday rotation ρ as functions of the field intensity. A characteristic feature of their behavior is the absence of a jumplike change in the field $H_{cr} = 182 \pm 9$ kOe at which singularities in the form of a kink are observed in the behavior of $\delta(H)$ and $\rho(H)$. The position of the plane of the optical axes is illustrated in Fig. 4. Within an error of $\pm 3°$, the optical axis remain in the (110) plane both at $H < H_{cr}$ and at $H > H_{cr}$. We note that the deviation of the axes from the (110) plane in weak fields is due to the presence of spontaneous elastic stresses in the sample, due to the conditions under which the single crystal was grown. In the absence of a magnetic field, the azimuthal angle of the plane of the optical axes, measured from the [100] direction, is close to $10°$. It is determined by the values of the spontaneous and artificially produced crystal strains along [110]. With increasing H, the plane of the optical axes turns towards the (110) plane. The spontaneous birefringence present in the sample because of the presence of the elastic stresses was not subtracted from the experimental data, since its effect is negligible in the strong-field region of interest to us.

The conoscopic method made it possible to determine δ with an absolute error at $H < H_{cr}$ of about ± 6 deg/mm, which amounts to $+6\%$ of the maximum measured value. In fields $H > H_{cr}$, where the contribution of the Faraday rotation is more substantial and measurements of the directions of the optical axes is difficult, the error increases to $\pm 15\%$. The error in the measurement of the Faraday rotation is approximately ± 15 deg/mm or $\pm 8\%$ of the maximum value. The random errors which
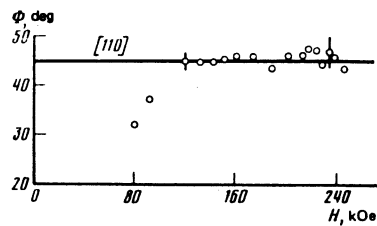
determine the scatter of the points are smaller than those cited by approximately a factor of 2.

To verify the obtained dependence of the Faraday rotation, additional measurements of the Faraday effect (FE) were performed in essentially inhomogeneous AFM samples. Since the linear birefringence is almost completely cancelled out when the sample is attached, because it breaks up into a large number of thin AFM domains, as is evidenced by its conoscopic figure which is typical of uniaxial crystals (Fig. 5), it is possible to measure the FE by usual methods without incurring exceesive systematic errors. Measurements in a thick sample ($l = 2.7$ mm), performed with light from a helium-neon laser at two directions of the field $H < H_{cr}$, yielded a $\rho(H)$ dependence that agreed (with allowance for the dispersion of the FE) with the data of Fig. 3b. The only oscillogram obtained from this sample also revealed a kink at $H \approx 182$ kOe, but the sample was damaged in a field of approximately 200 kOe. We note that damage to the samples was observed also in fields near 150 kOe. We used subsequently a relatively thin ($l = 0.45$ mm) sample, which remained single-domain in the magnetic field and was not damaged. A typical oscillogram, showing the change of the intensity of the linearly polarized light passing through an analyzer with an azimuth differing by $75°$ from the azimuth of the polarizer, is shown in Fig. 6a. The result of its reduction is shown in Fig. 6b. These experiments with multidomain samples confirm the presence of a kink on the plot of the FE against H at 182 kOe and the absence of any jumplike change of the rotation. We note also the absence of any noticeable hysteresis of the $\rho(H)$ curve.

4. DISCUSSION OF EXPERIMENTAL RESULTS

The main qualitative results of the experiments are the presence of kinks on the plots of $\delta(H)$ and $\rho(H)$ in a
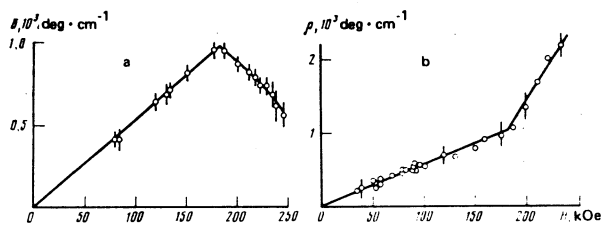

FIG. 3. Dependence of the linear birefringence (a) and of the Faraday rotation (b) reconstructed from the parameters of the conoscopic figures of a single-domain sample, on the intensity of the field $H \parallel C_4$.

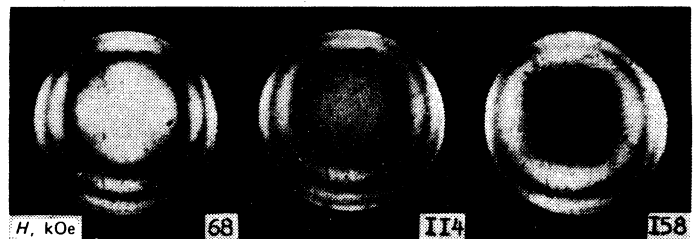FIG. 5. Conoscopic figures of multidomain sample vs. the intensity of the field $H \parallel C_4$; linearly polarized light (crossed polarizers), $\lambda = 4000$ Å, $t = 2.7$ mm.
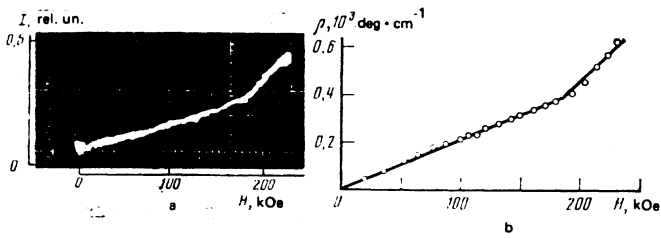
FIG. 6. Faraday rotation obtained by photoelectric measurements in a multidomain sample: a) typical oscillogram of the change of the intensity of the light and b) reconstructed dependence of the Faraday rotation, $\lambda = 6328$ Å.

field close to 182 kOe, and the absence of any jumplike changes in fields up to 250 kOe, as well as the fact that the samples were damaged only in those cases when the sample consisted of a set of AFM domains and was large enough.

1. These results indicate that in CoF_2 in a longitudinal magnetic field there is no first-order phase transition of the spin-flop type. This conclusion contradicts those of Refs. 4–7, but in the latter the main argument favoring the first-order transition was the fact that the sample was damaged, which was interpreted as the result of stratification into domains of collinear and spin-flop magnetic phases.

The results of the present study indicate that the damage is due to the elastic stresses that grow in the field in incoherent domain walls between the 180° AFM domains. These stresses are due linear magnetostriction whose sign is different for neighboring AFM domains.

2. From the experimental fact that in a field $H > H_{cr}$ the optical axes lie in the crystallographic plane (110) (Fig. 4) it follows that the strong-field noncollinear state of CoF_2 is described by the magnetic point group $2/m$, i.e., the vectors of the magnetic sublattice moments lie in the (110) plane. We note that the azimuthal angle Φ of the plane of the axes is quite sensitive to the position of the magnetic vectors. Using (10), we can express approximately the connection between the azimuthal angles of the plane of the optical axes and of the vector $l_\perp$ (the angle φ) by the relation

$$\text{tg}\, 2\Phi = (n_{x'x'} - n_{y'y'})\,[(n_{xx} - n_{yy})_\perp \cos 2\varphi]^{-1}.$$

where $(n_{x'x'} - n_{y'y'})$ is the observed birefringence at $H \sim H_{cr}$, and $(n_{xx} - n_{yy})_\perp$ is the maximum birefringence that can be due to the transverse components $l_\perp$ and $m_\perp$. The value of $(n_{xx} - n_{yy})_\perp$ can be estimated using the measured birefringence $(n_{xx} - n_{yy})$ at $H \parallel [100]$ (Ref. 14) and the estimated polar angle of the AFM vector in this field.[15] It turned out to be close to $3 \cdot 10^{-4}$. At a ratio $(n_{x'x'} - n_{y'y'})(n_{xx} - n_{yy})^{-1} \sim 0.3$ the error in the determination of the azimuth of the plane of the optical axes is approximately 3° and corresponds to an uncertainty less than 2° in the azimuthal angle of $l_\perp$.

3. The experimental $\rho(H)$ and $\delta(H)$ dependences can be used to determine the dependence of the angle of rotation of l away from the C_4 axis at $H > H_{cr}$. In the general case the expression for δ depends on the longitud-

inal and transverse projections of the FM and AFM vectors:

$$\delta = \frac{2\pi t}{\lambda \bar{n}} (Q_{66}^{ll} l_\perp^2 + Q_{66}^{mm} m_\perp^2 + 2Q_{61}^{ml} m_\perp l_\perp + 2Q_{63}^{ml} m_z l_z). \tag{12}$$

The magnetooptical constants Q_{66}^{mm}, Q_{66}^{ll}, Q_{61}^{ml} are unknown. The contribution of the transverse components can be experimentally estimated by performing an additional experiment at $H \parallel [110]$. In this case the symmetry of the magnetic subsystem will be the same, $2/m$, and the expression for the birefringence of the light propagating along $[001]$ will take the same form (12), but new $m_z \ll m_\perp$, since the longitudinal moment results only from the presence of fourth-order invariants of the type $g m_z l_x l_y l_z$ in the potential. Examination of the conoscopic figures at $H \parallel [100]$ and $H \parallel [110]$ in a field of approximately 30 kOe has shown that $(n_m - n_p)$ is smaller by one order at $H \parallel [110]$ than at $H \parallel [100]$, and amounts to approximately $10^{-6}k$, where $k = \pm(2 \pm 1)$. Recognizing that the induced projection of the AFM vector is $l_z \approx dm_z$, where $d = H_d/H_f$ and $m_\perp$ equals 0.1 in a field $H \parallel [110]$ of intensity 30 kOe (Ref. 7), we obtain

$$\frac{n_m - n_p}{m_\perp^2} = \frac{1}{\bar{n}} (d^2 Q_{66}^{ll} + 2d Q_{61}^{ml} + Q_{66}^{mm}) = 10^{-4}k. \tag{13}$$

At $H \parallel [001]$ in a field $H > H_{cr}$ the transverse magnetic moment $m_\perp = dl_\perp$, and since $(n_m - n_p) = 1.06 \cdot 10^{-4}$ and $m_z = 0.1$ at $H = H_{cr}$, it follows according to (8) that $Q_{63}^{ml}/\bar{n} = 10^{-3}$. Since the most important electronic optical transitions for birefringence are intense single-ion (or single-sublattice) transitions, for which $Q_{ij}^{ll} = Q_{ij}^{mm}$, it follows from (12) and (13) that the contributions of the components m_z and l_z to the birefringence at $H \parallel [001]$ will predominate at $10^{-4}k l_\perp^2 < 10^{-3} m_z l_z$ or, recognizing that $m_z \sim 0.1$, we have $k \sin\theta \tan\theta < 1$. At $k = 1$ we have $\theta < 50°$ and $l_z > 0.6$. The foregoing estimates point to a noticeable contribution (~ 0.25) of the transverse components already at $\theta \approx 30°$, or $l_z \approx 0.87$, and to the need for taking the contribution into account when determining the projections l_z. The $m_z(H)$ dependence is determined directly from the FR relation

$$\rho(H) = \frac{\pi t}{\lambda \bar{n}} f_{zyz}^m m_z(H). \tag{14}$$

To determine the scale for m_z, we used the values of the magnetic moment in fields $H < 182$ kOe from Ref. 7. Knowing m_z, putting $l_z^2 = 1 - l_z^2$, and using the numerical values (13) in the approximation of single-sublattice optical transitions for l_z, in accord with (12), we can write the equation

$$10^{-4}k(1 - l_z^2) + 10^{-3} m_z l_z = (n_{x'x'} - n_{y'y'}). \tag{15}$$

whose solution can yield l_z at $H > H_{cr}$. The decrease of the birefringence in a field $H < H_{cr}$ is evidence of opposing contributions of the longitudinal and transverse projections of m and l, i.e., $k < 0$. Figure 6 shows the obtained plots of $m_z(H)$ and the region of the possible values of $l_z(H)$. Of course, the obtained $l_z(H)$ is more readily qualitative than quantitative, since the small contribution of the transverse components was determined very approximately.

4. The possibility of experimentally determining the $m_z(H)$ and $l_z(H)$ dependence in CoF_2 raises the question
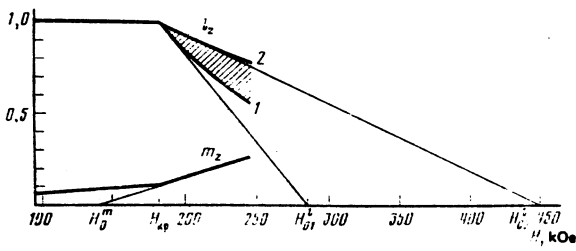
FIG. 7. Change of projections of the FM and AFM vectors as a function of the intensity of the field $H \parallel C_4$: curves 1 and 2 correspond to the parameter k [see (13)] equal to -1 and -3.

of theoretically describing the behavior of the sublattice moments in a field $H > H_{cr}$. The behavior of antiferromagnets whose thermodynamic potential contains the invariants $(m_x l_y + m_y l_x)$ and $l_x^2 l_y^2$ was considered in Ref. 2, where magnetic phase diagrams of the AFM were plotted in the (H, d) plane, analytic expressions were obtained for the coordinates of the singular points and lines on the diagrams, and the behavior of the magnetic properties was considered. These results, unfortunately, cannot be used for comparison with the present experiment, since that paper deals with the case of small d, when the change in the lengths of magnetic-moment vectors of the ions is neglected. In cobalt fluoride the influence of the single-ion rhombic anisotropy leads to such large changes in a longitudinal magnetic field $H \parallel C_4$, that the magnetic susceptibility χ_{zz} as $T \to 0$ K amounts to more than one-third of the susceptibility at the Néel point.[9] Since a rigorous solution of the quantum-mechanical problem, with account taken of the change of the ground state of the Co^{2+} ion in the field is difficult when the noncollinear phase is considered,[16,17] we have attempted to estimate the influence of these changes by using certain model dependences of the sublattice moments $M_i(H, \theta_i)$.

We regard the magnetic system of CoF_2 in the vicinity of the field H_{cr} as a ferrimagnetic system with sublattices $M_{1,2} = M_0 \pm \Delta M$, where $\Delta M = (1/2)M_z = (1/2)\chi_{zz} H_{cr}$. We assume that at $(H - H_{cr}) > 0$ the sublattice moments remain constant. This problem of the behavior of an axial ferrimagnet with rhombic single-ion anisotropy is also for independent interest. We confine ourselves in the thermodynamic potential to second-order invariants and express the potential in the form

$$\Phi = -I_{12} M_1 M_2 + K(M_1^2 + M_2^2) + D(M_{1x} M_{1y} - M_{2x} M_{2y}) - H(M_1 + M_2). \quad (16)$$

Such a potential allows an angular noncollinear state with sublattice-moment vectors lying in the (110) plane.[1] Introducing the notation $\Delta m = \Delta M / M_0$, $\varkappa = K / I_{12}$, $d = D / I_{12}$, and $h = H / I_{12} M_0$, and considering the class of solutions at $H \parallel C_4$ with M_i located in the (110) plane, we obtain in polar coordinates for the potential (16)

$$\Phi = -(1-\Delta m^2) \cos 2\zeta + 2\varkappa (1+\Delta m^2)(\cos^2\theta \cos^2\zeta + \sin^2\theta \sin^2\zeta)$$
$$+ 2\varkappa\Delta m \sin 2\zeta \sin 2\theta + 2d\Delta m(\sin^2\theta \cos^2\zeta + \cos^2\theta \sin^2\zeta)$$
$$- \tfrac{1}{2}d(1+\Delta m^2) \sin 2\theta \sin 2\zeta - 2h(\Delta m \cos\theta \cos\zeta + \sin\theta \sin\zeta). \quad (17)$$

Here $\theta = (1/2)(\theta_1 + \theta_2)$ and $\zeta = (1/2)(\theta_2 - \theta_1)$, where θ_1 and $\pi + \theta_2$ are the angles between the directions of $H \parallel C_4$ and M_1 and M_2. Confining ourselves to small

sublattice kink angles $2\zeta \ll 1$ or to small fields $H \ll H_{exc}$, we obtain from the condition for the compatibility of the equations $\partial\Phi/\partial\zeta = 0$ and $\partial\Phi/\partial\theta = 0$ an equation that connects the field intensity and the angle of rotation of the magnetic moments:

$$\begin{vmatrix} a & b \\ c & d \end{vmatrix} = 0, \quad (18)$$

$a = 2(1 - \varkappa \cos 2\theta) + h\Delta m \cos\theta + 2d\Delta m \cos 2\theta - 2\Delta m^2(1 + \varkappa \cos 2\theta)$,
  $b = -h - d\cos\theta + 4\varkappa\Delta m \cos\theta - d\Delta m^2 \cos\theta$,
  $c = -h\cos\theta - d\cos 2\theta + 4\varkappa\Delta m \cos 2\theta - d\Delta m^2 \cos 2\theta$,
  $d = -2\varkappa \cos\theta + h\Delta m + 2d\Delta m \cos\theta - 2\varkappa\Delta m^2 \cos\theta$.

Letting θ tend to zero, we obtain an equation for the field at which the collinear phase loses lability

$$h_{cr} = [-4\varkappa(1-\varkappa) + \Delta m^2 - 2\Delta md(1+2\varkappa)]^{1/2} + \Delta m(1+2\varkappa) - d \quad (19)$$

or

$$H_{cr} = \left[H_A(2H_E + H_A) + \left(\frac{\Delta M}{M_0}\right)^2 H_E^2 - 2\frac{\Delta M}{M_0} H_D(H_E - H_A) \right]^{1/2}$$
$$+ \frac{\Delta M}{M_0}(H_E - H_A) - H_D. \quad (20)$$

where $H_E = I_{12} M_0$, $H_A = -2K M_0$, $H_D = D M_0$ or $\varkappa = -H_A/2H_E$ and $d = H_D/H_E$. As $H_A \to 0$ and $H_D \to 0$ Eq. (20) goes over into the expression for the critical field of the transition of an isotropic ferrimagnet into the canted state, $H_{cr} \to 2\Delta M H_E / M_0$, and as $H_D \to 0$ and $H_A \to 0$ it agrees with the expression for the field of the kink of the sublattices of a ferrimagnet with uniaxial anisotropy.[18,19] At $\Delta m = 0$ it coincides with the corresponding expression of Ref. 2:

$$h_{cr}(\Delta m=0) = [-4\varkappa(1-\varkappa)]^{1/2} - d. \quad (21)$$

From (18) we can obtain an expression for the derivative $d\cos\theta/dh$ at the point $h = h_{cr}$. If the distance between the magnetic moments of the sublattices is not very large and the condition $\Delta m^2 \ll 1$ holds, then

$$\left(\frac{d\cos\theta}{dh}\right)_{cr} = -\frac{h_{cr} + d - \Delta m(1+2\varkappa)}{2d(h_{cr} + d) - 8\varkappa^2 + \Delta m h_{cr}(1-4\varkappa)}. \quad (22)$$

Expression (22) can be represented in the form

$$\left(\frac{d\cos\theta}{dh}\right)_{cr} = -\frac{1-\alpha}{2(1-\beta)(d-d_{cr})} = -\frac{1}{h_0' - h_{cr}}, \quad (23)$$

where

$\alpha = \Delta m(1+2\varkappa)/h_1,$ $\beta = \Delta m(1-4\varkappa)/2h_1,$ $h_1 = h_{cr} + d \approx [-4\varkappa(1-\varkappa)]^{1/2},$
  $d_{cr} = d_{cr1} \dfrac{1 - \Delta m(1-4\varkappa)/2d_{cr1}}{1-\beta},$ $d_{cr1} = \dfrac{4\varkappa^2}{h_1},$ $\quad (24)$

h_0' is the field at which the tangent crosses the abscissa axis.

At d, $\varkappa \neq 0$, and $\Delta m = 0$, the coefficients α, $\beta = 0$ and $h_1 = [4\varkappa(1 - \varkappa)]^{1/2}$, and expression (23) simplifies to:

$$\left(\frac{d\cos\theta}{dh}\right)_{cr0} = -\frac{1}{2(d-d_{cr0})}, \quad (25)$$

where

$$d_{cr0} = -2\varkappa \left(-\frac{\varkappa}{1-\varkappa}\right)^{1/2} \approx d_{cr}. \quad (26)$$

At a rhombic-anisotropy constant $d = d_{cr}$ the tangent to the plot of $\cos\theta = f(h)$ at the point $h = h_{cr}$ is vertical, and at $d < d_{cr}$ the function $f(h)$ is not single-valued. Under these conditions, the noncollinear state with $\theta \to 0$ does

not correspond to a minimum of the potential (17), and the transition from the collinear state into the canted state can take place only via a first-order phase transition.

In the case d, $\varkappa = 0$, $\Delta m \neq 0$, Eq. (22) goes over into the corresponding expression for an isotropic ferrimagnet:

$$\left(\frac{d\cos\theta}{dh}\right)_{cr\ FM} = -\frac{1}{2\Delta m}. \tag{27}$$

At $\Delta m \ll 1$ the slope of the tangent to the plot of $\cos\theta = f(h)$ at the point $h = h_{cr}$ decreases both because of the decrease of the effective parameter d_{cr} and by virtue of the appearance of a small correction α in (23). At sufficiently large $\Delta m > 8\varkappa^2/h_1(1 - 4\varkappa)$ the transition to the noncollinear state is of second order also at $d = 0$. Of course, in the considered AFM, Δm and d are not independent quantities. Changes of the sublattice magnetic moments of the AFM are impossible at $d = 0$. The difference Δm is a complicated function of d, $\varkappa$, and h (Ref. 17), but since Δm can be determined from experiment, the expressions (18)–(23) above, in which Δm enters as an independent parameter, can be useful in the reduction of the experimental results.

In addition to the quantity $(d\cos\theta/dh)_{cr}$, it is easy to determine in experiment also the function $m_z(h)$, which is close to linear. In the considered model with $M_1-M_2 = \text{const}$ it can be seen that

$$m_z = 2\Delta m\cos\theta + 2\zeta\sin\theta. \tag{28}$$

The sublattice kink angle 2ζ is determined from the condition that the potential (17) be a minimum. Confining ourselves to the linear approximation, we obtain in the case $\Delta m^2 \ll 1$

$$m_z = 2\Delta m + 2\Delta m(1-\gamma)\frac{h-h_{cr}}{h_0'-h_{cr}}, \tag{29}$$

where

$$\gamma = \frac{h_{cr}+d-4\varkappa\Delta m}{\Delta m(1-\varkappa+\frac{1}{2}h_{cr}\Delta m+d\Delta m)}.$$

The straight lines $l_z'(H) = 1 - \Delta hd\cos\theta/dh$ and $m_z'(H)$ have on the abscissa axis intercepts

$$h_0'-h_{cr} = \frac{2(d-d_{cr})(1-\beta)}{1-\alpha} \text{ and } h_{cr}-h_0^m, \tag{30}$$

whose ratio is

$$(h_0'-h_{cr})/(h_{cr}-h_0^m) = \gamma-1. \tag{31}$$

The obtained expressions (20), (23), (30), (31) make it possible to determine the values of the effective fields $H_{D_{cr}}$, H_D, H_E, and H_A. For CoF_2 these expressions can be simplified without introducing an error larger than 10% at H_D, $H_A < (1/2)H_E$, recognizing that $\Delta M/M_0 = 0.1$, and they can be rewritten in the form

$$H_{D\ cr} = \frac{H_A[H_A(2H_E+H_A)]^{1/2}}{2H_E+H_A}\left(1-\Delta m\frac{[H_A(2H_E+H_A)]^{1/2}(H_E+2H_A)}{2H_A^2}\right), \tag{32}$$

$$H_{cr} = [H_A(2H_E+H_A)]^{1/2}-H_D+(\Delta M/M_0)(H_E-H_A), \tag{33}$$

$$H_D = \frac{1}{2}(H_0'-H_{cr})+H_{Dcr} \tag{34}$$

$$\frac{H_0'-H_{cr}}{H_{cr}-H_0^m} = \frac{2(H_{cr}+H_D)}{\Delta m(2H_E+H_A)} - 1. \tag{35}$$
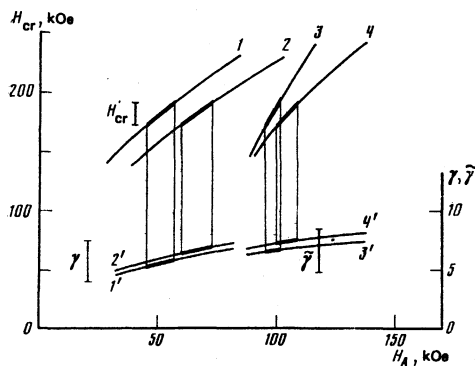

FIG. 8. Comparison of the experimental determined values of the critical field (1–4) and of the parameters γ and $\bar{\gamma}$ (1'–4') for two models of the behavior of the magnetic system of CoF_2 [1,2 $-\Delta m(\theta) = \text{const}$ and 3,4 $-\Delta m(\theta) = \Delta m_0\cos\theta$)] as functions of H_A and H_E ($2H_E$[kOe] = 800 (1,1'), 700 (2,2'), 1500 (3,3'), 1200 (4,4')). The thick sections of the lines correspond to the regions of the permissible values of H_A at specified $2H_E$ and the experimental tolerances for H_{cr} and γ, also marked on the figure.

The order of magnitude of the error incurred in the determination of H_D is close to $(\Delta M/M_0)(2H_E - H_A)$ $(H_{cr} - H_D)^{-1}$, and that in H_{cr} is close to

$$(\Delta M/M_0)(H_D/H_A)(H_E-H_A)(2H_E+H_A)^{-1}.$$

The experimentally determined values of the characteristic fields are $H_{cr} = 182$ kOe, $H_0^m = 140$ kOe, $H_0^l = 290$–450 kOe, and $(H_0^l - H_{cr})(H_{cr} - H_0^m)^{-1} = 5 \pm 2$. By varying the values of the fields H_E and H_A it is possible to obtain the best agreement between these values and the calculated ones. The results of the calculation are shown in Fig. 8.

The agreement of the experimental data with one another is reached within the framework of the model at $2H_E = 800$ kOe, $H_A = 50$ kOe, and $H_D = 54$ kOe.

The obtained values of the effective fields differ from those employed for the phenomenological description of their resonant and magnetic properties: for example, $2H_E = 700$ kOe, $H_A = 120$ kOe, $H_D = 240$ kOe in Ref. 6 and $2H_E = 480$ kOe, $H_A = 75$ kOe, $H_D = 115$ kOe in Ref. 8. Just as the other sets of effective fields, the obtained set, apart from the exchange constant, does not agree with the energy parameters in the spin Hamiltonian used in the quantum-mechanical description of the properties of CoF_2 (Ref. 9). The discrepancy is not surprising, since the analysis presented in the present paper is highly approximate. A more rigorous approach calls for allowance for the spin of the ion as a function of its orientation in the crystal, for the change of the effective field acting in the collinear phase on the Co^{2+} ion, and for the anisotropy of the g-factor. Some results that take into account the change of the spin state at a result of quantum-mechanical mixing of the states were obtained in Refs. 16 and 17. However, the behavior of the canted ($\theta \neq \pi/2$) noncollinear phase, which is precisely the state realized in CoF_2 at $H > H_{cr}$, is not considered in these references. Allowance for all the changes of the properties of the Co^{2+} ion in the canted phase is difficult. We have estimated the influence of the dependence of the field-induced increments

to the sublattice magnetic moments on the angle θ_i. Putting

$$\Delta M_i = \Delta M(H = H_{cr}) \cos \theta_i \qquad (36)$$

and analyzing the potential (17), we obtained expressions for h_{cr} and $d\cos\theta/dh$. Since the equations are complicated, we write down only the first terms of their expansions in Δm. The expression for the critical field

$$\hbar_{cr} = [-4\varkappa(1-\varkappa) - 2\Delta m^2 + 24\Delta m^2 \varkappa]^{1/2} - d + \Delta m(1+2\varkappa) \qquad (37)$$

differs little from the preceding one at $|4\varkappa(1-\varkappa)| \gg \Delta m^2$, while the dependence of the rotation angle on H and effective critical field of rhombic anisotropy change appreciably

$$\left(\frac{\widetilde{d\cos\theta}}{dh}\right)_{cr} = \frac{1-\tilde{\alpha}}{2(1-\tilde{\beta})(d-\tilde{d}_{cr})}, \qquad (38)$$

where $\tilde{\alpha} \approx \alpha$, $\tilde{\beta} = \Delta m(4+\varkappa)/h_1$, $h_1 = h_{cr} + d$, and

$$\tilde{d}_{cr} = d_{cr1}\frac{1 - 2\Delta m\varkappa/d_{cr1}}{1-\beta}. \qquad (39)$$

Accordingly, the field intervals between the tangents to the plots of $\cos\theta$ and m_z against h at the point $h = \bar{h}_{cr}$ are equal to

$$\hbar_0' - h_{cr} = 2\frac{1-\beta}{1-\alpha}(d-\tilde{d}_{cr}), \quad \frac{\hbar_0' - \hbar_{cr}}{\hbar_{cr} - \hbar_0'''} = \bar{\gamma} - 2, \qquad (40)$$

where

$$\bar{\gamma} = \frac{\hbar_1 + \Delta m(1-6\varkappa)}{(1-\varkappa+\Delta m\hbar_1)\Delta m}. \qquad (41)$$

The calculation results obtained in this approximation are also shown in Fig. 8. The experimental values can be reconciled in this model at large values of the exchange and anisotropic interactions: $2H_E = 1500$ kOe, $H_A = 100$ kOe, and $H_D = 275$ kOe. The strong dependence of the effective fields on the model of the behavior of the sublattice moments demonstrates the need for a more rigorous allowance for the changes of $M_i(\theta_i)$ in a quantitative description of the noncollinear structure of cobalt fluoride.

5. CONCLUSION

Measurement of the circular and linear birefringences of the AMF cobalt fluoride as functions of the magnetic field intensity have led to the conclusion that CoF_2 is a typical representative of tetragonal crystals with sufficiently large single-ion rhombic magnetic anisotropy $d > d_{cr}$, which makes impossible an abrupt transition of the spin-flop type into a canted ($\theta \neq \pi/2$) noncollinear state. This transition is of second order and is not accompanied by destruction of the sample, provided that the sample is in a single-domain AFM state. The observed destriction of the samples is due to elastic stresses produced in concoherent 180° AFM domain walls in a magnetic field because of linear magnetostriction.

The phenomenological analysis shows that the behavior of the magnetic subsystem of CoF_2 can be qualitatively described by a potential in which the change of the sublattice magnetic moments in the noncollinear phase is neglected and it is assumed that $\Delta M = \Delta M(H = H_{cr})$. It was also shown that better agreement with experiment can be obtained by taking into account the dependence of the sublattice magnetic moments and their changes in the field on the orientation relative to the crystallographic axes.

[1] The state $\bar{1}$, at which M_i does not lie in the (110) plane, is possible only at sufficiently large anisotropy of the type $fl_x^2 l_y^2$ and $f > 0$.

[1] E. A. Turov, Fizicheskie svoistva magnitouporyadochennykh kristallov (Physical Properties of Magnetically Ordered Crystals), AN SSSR, 1963, p. 130 [Academic, 1965].

[2] V. S. Kuleshov and V. A. Popov, Fiz. Tverd. Tela (Leningrad) 15, 937 (1973) [Sov. Phys. Solid State 15, 652 (1973)].

[3] Yu. G. Litvinenko and V. V. Shapiro, Fiz. Nizk. Temp. 2, 233 (1976) [Sov. J. Low Temp. Phys. 2, 116 (1976)].

[4] V. I. Ozhogin, Candidate's dissertation, Inst. Phys. Problems, USSR. Acad. of Sci., Moscow, 1965.

[5] K. N. Kocharyan and E. G. Rudashevskii, Izv. AN SSSR, ser. fiz. 36, 1556 (1972).

[6] K. N. Kocharyan, Candidate's dissertation, Inst. Phys. Problems USSR Acad. Sci., 1973, p. 107.

[7] V. G. Shapiro, V. I. Ozhogin, and K. T. Gurtovoi, Izv. AN SSSR, ser. fiz. 36, 1559 (1972).

[8] K. T. Gurtovoi, Fiz. Tverd. Tela (Leningrad) 20, 2666 (1978) [Sov. Phys. Solid State 20, 1539 (1978)].

[9] M. E. Lines, Phys. Rev. 137A, 982 (1965).

[10] S. J. Allen and H. J. Guggenheim, Phys. Rev. B4, 4, 950 (1971).

[11] A. S. Prokhorov and E. G. Rudashevskii, Pis'ma Zh. Eksp. Teor. Fiz. 10, 175 (1969) [JETP Lett. 10, 110 (1969)].

[12] N. F. Kharchenko, V. V. Eremenko, and L. I. Belyi, ibid. 29, 432 (1979) [29, 392 (1979)].

[13] J. F. Nye, Physical Properties of Crystals, Oxford, 1957, Russ. transl. IIL, 1960, p. 315.

[14] A. S. Borovik-Romanov, N. M. Kreines, A. A. Pankov, and M. A. Talalaev, Zh. Eksp. Teor. Fiz. 64, 1762 (1973) [Sov. Phys. JETP 37, 890 (1973)].

[15] V. I. Ozhogin, Doctoral dissertation, Kurchatov Institute, Moscow, 1974, p. 79.

[16] V. S. Ostrovskii and V. M. Loktev, Preprint ITF-77-105R, 1977.

[17] V. M. Loktev and V. S. Ostrovskii, Fiz. Tverd. Tela (Leningrad) 20, 3257 (1978) [Sov. Phys. Solid State 20, 1878 (1978)].

[18] V. V. Eremenko and N. F. Kharchenko, Phase Trans. 1, 61 (1979).

[19] V. G. Bar'yakhtar, E. P. Stefanovskii, and D. A. Yablonskii, Fiz. Met. Metallov. 42, 684 (1976).

[20] Yu. I. Sirotin and M. P. Shaskol'skaya, Osnovy kristallofiziki (Principles of Crystal Physics), M., Nauka, 1979, p. 617.

Translated by J. G. Adashko